J Electr Eng Technol.2017; 12(5): 1991-2000
http://doi.org/10.5370/JEET.2017.12.5.1991

ISSN(Print) 1975-0102
ISSN(Online) 2093-7423

Compensative Microstepping Based Position Control with Passive Nonlinear Adaptive Observer for Permanent Magnet Stepper Motors

Wonhee Kim*, Youngwoo Lee, Donghoon Shin*** and Chung Choo Chung†**

Abstract – This paper presents a compensative microstepping based position control with passive nonlinear adaptive observer for permanent magnet stepper motor. Due to the resistance uncertainties, a position error exists in the steady-state, and a ripple of position error appears during operation. The compensative microstepping is proposed to remedy this problem. The nonlinear controller guarantees the desired currents. The passive nonlinear adaptive observer is designed to estimate the phase resistances and the velocity. The closed-loop stability is proven using input to state stability. Simulation results show that the position error in the steady-state is removed by the proposed method if the persistent excitation conditions are satisfied. Furthermore, the position ripple is reduced, and the Lissajou curve of the phase currents is a circle.

Keywords: Permanent magnet stepper motor, Microstepping, Adaptive control

1. Introduction

Microstepping has been widely used for improved resolution and significantly increased motion stability for position control of permanent magnet (PM) stepper motor [1-3]. Microstepping largely eliminates the jerks that appear with full or half-stepping, and prevents speed reversal [2]. However, in microstepping without feedback control (open-loop microstepping), the phase currents are decreased and experience phase lag due to back-emfs and phase inductances during operation. Therefore, proportional and integral (PI) current feedback is widely used to compensate the phase currents in industrial applications [3-6]. If the bandwidth of the designed PI current feedback loop is much greater than the maximum velocity, the effect of the back-emf may be negligible. However, poor transient performance exists in the position control.

Position feedback by resolvers or encoders built into PM stepper motors was previously used to improve microstepping in industrial applications [7, 8]. Various feedback control methods have been implemented to improve the performance of the position control of microstepping [9-13]. Recently, several advanced microstepping methods were developed to improve the position tracking performance of the microstepping [14, 15]. In previous researches [9-17], it was assumed that the resistances of phases A and B had the same value. However, the phase resistances may be unknown due to mechanical errors so that the phase resistances are different [18]. The tolerance of the resistance in industry is generally ±10% [18]. The phase resistance may vary during operation [19]. In [19], the adaptive algorithm to estimate the resistance was proposed. However, the adaptive algorithm can estimate only resistance without the angular velocity. Thus it requires the velocity sensor. Furthermore, it was also assumed that both resistance of phase A and B are same. When the phase resistances of phases A and B are different, both ripple and offset error in the position cannot be compensated for by current control method based on conventional microstepping, i.e., PI controller or nonlinear controller. Thus, the control method to solve the problem should be developed. And the estimation method is required to estimate the different phase resistances and the velocity. Several adaptive observers were proposed [20], but there was no one to estimate the velocity, and phase A and B resistances for the PM stepper motor.

In this paper, a compensative microstepping based position control with passive nonlinear adaptive observer is proposed for position tracking in PM stepper motor when the phase resistances are different. Lissajous curve is the graph of a system of parametric equations which describe complex harmonic motion. If the phase resistances are different, the Lissajou curve of the desired phase currents used in the previous methods [11, 12] becomes an ellipse. Therefore, a position error exists in the steady-state, and ripple of position errors appear during operation. To resolve this problem, a compensative microstepping is designed to make the Lissajou curve of the desired phase currents become a circle. To ensure that the phase currents follow the desired paths during operation, the nonlinear control is used [11, 12]. The integral action is used to eliminate steady-state errors due to dc offsets in the current

† Corresponding Author: Division of Electrical and Biomedical Engineering, Hanyang University, Korea. (cchung@hanyang.ac.kr)
* School of Energy Systems Engineering, Chung-Ang University, Korea. (whkim79@cau.ar.kr)
** Department of Electrical and Computer Engineering, UNIST and Department of Mechanical Engineering, University of California, Berkeley. (stork@unist.ac.kr)
*** Global R&D Center, MANDO Corporation, Korea. (donghoon.shin @halla.com)
Received: May 22, 2017; Accepted: June 16, 2017

measurement. A passive nonlinear adaptive observer is also designed to estimate the phase resistances and the velocity. To the best of the authors' knowledge, it might be the first attempt of the design of the adaptive observed to estimate the velocity, and phase A and B resistances for the PM stepper motor. The closed-loop stability is proven using input to state stability. Simulation results show that the steady-state position error disappears and the ripple is reduced through the use of the proposed method. Furthermore, the proposed method returns Lissajou curve of the phase currents to a circle under the different phase resistances.

2. Mathematical Model of PM Stepper Motor and Compensative Mocristepping

2.1. Mathematical model of PM stepper motor

A PM stepper motor consists of a slotted stator with two phases and a permanent magnet rotor which has north and south poles. Detailed description of the operation of PM stepper motor is presented in [21, 22]. The dynamics of PM stepper motor can be represented in the state-space form $\dot{x} = f(x,u)$ as follows [21-23]:

$$\begin{aligned}\dot{\theta} &= \omega \\ \dot{\omega} &= \frac{1}{J}\left[-K_m i_a \sin(N_r\theta) + K_m i_b \cos(N_r\theta) - B\omega\right] \\ \dot{i}_a &= \frac{1}{L}\left[v_a - Ri_a + K_m\omega\sin(N_r\theta)\right] \\ \dot{i}_b &= \frac{1}{L}\left[v_b - Ri_b - K_m\omega\cos(N_r\theta)\right]\end{aligned} \tag{1}$$

where $x = [\theta,\omega,i_a,i_b]^{\mathrm{T}}$ is a vector of state variables and $u = [v_a,v_b]^{\mathrm{T}}$ is a vector of inputs. v_a, v_b and i_a, i_b are the voltages [V] and currents [A] of phases A and B, respectively. θ is the rotor (angular) position [rad], ω is the rotor (angular) velocity [rad/s], B is the viscous friction coefficient [N·m·s/rad], J is the inertia of the motor [Kg·m^2], K_m is the motor torque constant [N·m/A], R is the resistance of the phase winding [Ω], L is the inductance of the phase winding [H], and N_r is the number of rotor teeth.Vsis the supplied voltage of PM stepper motor. The parameters of PM stepper motor are shown in Table 1 [24]. The position and phase currents are measurable.

2.2. Compensative microstepping

In [12], the stability of microstepping was proven using Lyapunov method.

Theorem 1: Consider the PM stepper motor (1). Suppose that the microstepping inputs v_a^d and v_b^d are given to PM stepper motor (1) as

$$v_a^d = V_{\max}\cos(N_r\theta^d), \quad v_b^d = V_{\max}\sin(N_r\theta^d) \tag{2}$$

where θ^d is the constant desired position and $V_{\max}$ is the amplitude of the input voltage. Then the state x of the PM stepper motor (1) locally converges to an equilibrium point $x_e = \left[\theta^d, 0, i_a^d, i_b^d\right]^T$, that is,

$$\begin{aligned}&\lim_{t\to\infty}\theta(t) = \theta^d, \lim_{t\to\infty}\omega(t) = 0 \\ &\lim_{t\to\infty} i_a(t) = i_a^d, \lim_{t\to\infty} i_b(t) = i_b^d\end{aligned} \tag{3}$$

where

$$i_a^d = \frac{v_a^d}{R}, i_b^d = \frac{v_a^d}{R} \tag{4}$$

are the desired currents for microstepping. ♦

In general, it is assumed that the resistances in phase A and B, R_a and R_b, are equal to R, which allows the desired current vector to form a circle, as shown in Fig. 1.

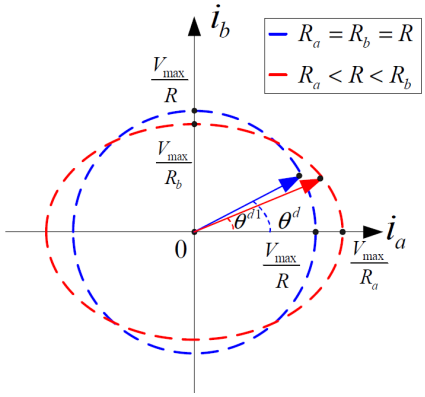

Fig. 1. Lissajou curves of phase currents of the two cases

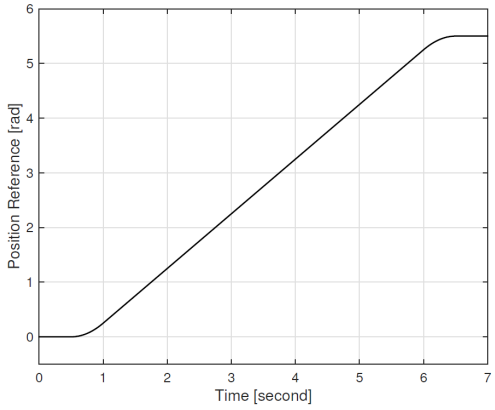

Fig. 2. Reference position

Table 1. Stepper motor parameters

Parameter	Value	Parameter	Value
L	0.040	V_s	24
R_a	14.06	R_b	15.54
J	3×10^{-5}	K_m	0.165
N_r	50	B	8×10^{-4}

However, R_a and R_b are actually different, causing the phase currents to be plotted as an ellipse, as shown in Fig. 1. Therefore, the position error appears as

$$\operatorname{atan}\left(\frac{R_a V_{\max}\sin\left(N_r\theta^d\right)}{R_b V_{\max}\cos\left(N_r\theta^d\right)}\right)=\theta^{d1}\neq\theta^d \tag{5}$$

In Fig. 1, the magnitude of the position error varies with the electrical degree of the desired position. This position tracking error produces a ripple during operation. Therefore, we propose the compensative microstepping such as

$$v_a^d=\frac{2R_a V_{\max}}{R_a+R_b}\cos\left(N_r\theta^d\right), v_b^d=\frac{2R_b V_{\max}}{R_a+R_b}\sin\left(N_r\theta^d\right). \tag{6}$$

Then both desired currents becomes

$$i_a^d=\frac{2V_{\max}}{R_a+R_b}\cos\left(N_r\theta^d\right), i_b^d=\frac{2V_{\max}}{R_a+R_b}\sin\left(N_r\theta^d\right). \tag{7}$$

Remark 1: Although (2) is changed into (6) in microstepping, the stability of microstepping holds since only the amplitude of the (2), $V_{\max}$ is changed into $\frac{2R_a V_{\max}}{R_a+R_b}$ and $\frac{2R_b V_{\max}}{R_a+R_b}$. ♦

When R_a = 13.32 Ω (−10%), R_b = 16.28 Ω (+10%), and $V_{\max}$=24 V, two types of open-loop microsteppings (normal microstepping (2) and compensative micro-stepping (6)) are compared by tracking the reference position shown in Fig. 2. The parameters in Table 1 are used for the simulations. Fig. 3 shows that the position steady-state position error appeared due to the different phase resistances. Furthermore, the ellipse Lissajou curves resulted in the increasing position ripple. The steady-state position error was not observed using (6), as shown in Fig. 3; however, since the current dynamics are affected by the different phase resistances, the ripple is reduced during operation when using open-loop compensative microstepping.

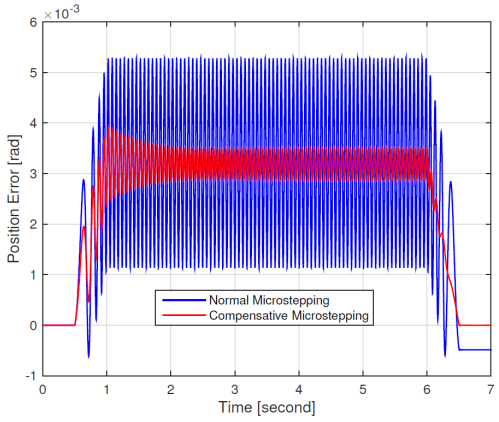

(a) Position tracking error

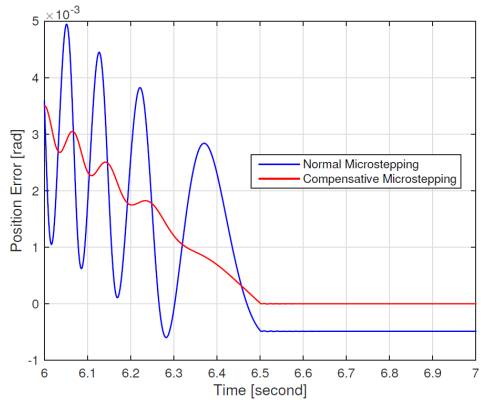

(b) Zoom of the position tracking error

Fig. 3. Tracking errors of two microstepping: micro-stepping and compensative microstepping

3. Controller and Observer Designs

3.1. Nonlinear controller

Using the compensative desired phase voltages (6) and currents (7), the current error and the integral of the current error are defined as

$$\begin{aligned} e_{a_I}(t)&=\int_0^t e_a(\tau)d\tau,\ e_a(t)=i_a^d(t)-i_a(t)\\ e_{b_I}(t)&=\int_0^t e_b(\tau)d\tau,\ e_b(t)=i_b^d(t)-i_b(t)\end{aligned} \tag{8}$$

Note that a dc current offset may appear in current measurements. The integral action is used to eliminate steady-state errors due to dc offsets in the current measurement. The phase voltage inputs are designed as

$$\begin{aligned} v_a&=\left(R_a i_a-K_m\omega\sin\left(N_r\theta\right)\right)+L\left(\dot{i}_a^d+\rho_{a_I}e_{a_I}+\rho_a e_a\right)\\ v_b&=\left(R_b i_b+K_m\omega\cos\left(N_r\theta\right)\right)+L\left(\dot{i}_b^d+\rho_{b_I}e_{b_I}+\rho_b e_b\right)\end{aligned} \tag{9}$$

where ρ_{a_I}, ρ_a, ρ_{b_I}, and ρ_b are control gains. The control gains are chosen such that are chosen such that the polynomials $s^2+\rho_{a_I}s+\rho_a$ and $s^2+\rho_{b_I}s+\rho_b$ are Hurwitz.

Theorem 2: Consider PM stepper motor (1). The control inputs (9) guarantee that e_{a_I} e_a, e_{b_I}, and e_b exponentially converge to zero as t → ∞. ♦

Proof: Consider a Lyapunov candidate function V_1 as

$$V_1=\frac{1}{2}e_{a_I}^2+\frac{1}{2}e_a^2+\frac{1}{2}e_{b_I}^2+\frac{1}{2}e_b^2. \tag{10}$$

Differentiating V_1 with respect to time yields

$$\begin{aligned}\dot{V}_1 &= e_{a_1}e_a + e_a\left(\dot{i}_a^d - \dot{i}_a\right) + e_{b_1}e_b + e_b\left(\dot{i}_b^d - i_b\right)\\ &= e_{a_1}e_a + e_{b_1}e_b\\ &\quad + e_a\left(\dot{i}_a^d - \frac{1}{L}\left(v_a - R_a i_a + K_m\omega\sin\left(N_r\theta\right)\right)\right)\\ &\quad + e_b\left(\dot{i}_a^d - \frac{1}{L}\left(v_a - R_a i_a - K_m\omega\sin\left(N_r\theta\right)\right)\right).\end{aligned} \tag{11}$$

With the control law (9), $\dot{V}_1$ is negative definite as

$$\dot{V}_1 = -\begin{bmatrix} e_{a_1}\\ e_a\\ e_{b_1}\\ e_b\end{bmatrix}^T \underbrace{\begin{bmatrix} 0 & 1 & 0 & 0\\ \rho_{a_1} & \rho_a & 0 & 0\\ 0 & 0 & 0 & 1\\ 0 & 0 & \rho_{b_1} & \rho_b\end{bmatrix}}_{A_e}\begin{bmatrix} e_{a_1}\\ e_a\\ e_{b_1}\\ e_b\end{bmatrix}. \tag{12}$$

Since A_e is Hurwitz, e_a and e_b exponentially converge to zero as t → ∞. ■

Notice that the Lyapunov-based control law (9) only guarantees local exponential stabilities of the desired currents i_a^d and i_b^d required for microstepping/

3.2. Passive nonlinear adaptive observer design

The phase resistances may be unknown due to mechanical errors [18]; furthermore, the phase resistance may vary during operation [19]. Thus, the resistances of phases A and B are not the same, and R_a and R_b need to be estimated. The Lyapunov-based controller (9) design assumed that the full state was known. However, we are unable to determine a velocity based on the simple backward Euler method, $\omega(kT) = [\theta(kT)-\theta(k-1)T]/T$ due to the resolution limit when the PM stepper motor operates at a low velocity. Therefore, an adaptive observer to estimate ω, R_a, and R_b is designed. The PM stepper motor dynamics (1) can be rewritten as

$$\begin{aligned}\dot{x} &= A(\theta)x + \phi_a\left(i_a\right)R_a + \phi_b\left(i_b\right)R_b + Bu\\ y &= Cx\end{aligned} \tag{13}$$

where

$$A(\theta) = \begin{bmatrix} 0 & 1 & 0 & 0\\ 0 & -\frac{B}{J} & -\frac{K_m}{J}\sin\left(N_r\theta\right) & \frac{K_m}{J}\cos\left(N_r\theta\right)\\ 0 & \frac{K_m}{L}\sin\left(N_r\theta\right) & 0 & 0\\ 0 & -\frac{K_m}{L}\cos\left(N_r\theta\right) & 0 & 0\end{bmatrix}$$

$$\phi_a\left(i_a\right) = \begin{bmatrix} 0\\ 0\\ -\frac{i_a}{L}\\ 0\end{bmatrix},\ \phi_b\left(i_b\right) = \begin{bmatrix} 0\\ 0\\ 0\\ -\frac{i_b}{L}\end{bmatrix}$$

$$B = \begin{bmatrix} 0 & 0\\ 0 & 0\\ \frac{1}{L} & 0\\ 0 & \frac{1}{L}\end{bmatrix},\ C = \begin{bmatrix} 1 & 0 & 0 & 0\\ 0 & 0 & 1 & 0\\ 0 & 0 & 0 & 1\end{bmatrix}.$$

As a result, a nonlinear observer is designed by

$$\dot{\hat{x}} = A(\theta)\hat{x} + \phi_a\left(i_a\right)\hat{R}_a + \phi_b\left(i_b\right)\hat{R}_b + Bu + L_{ob}C\left(x - \hat{x}\right) \tag{14}$$

where

$$L_{ob} = \begin{bmatrix} l_\theta & 0 & 0\\ l_\omega & 0 & 0\\ 0 & l_a & 0\\ 0 & 0 & l_b\end{bmatrix}$$

$\hat{x} = \left[\hat{\theta},\ \hat{\omega},\ \hat{i}_a,\ \hat{i}_b\right]^T$ is estimated x, $\hat{R}_a$ and $\hat{R}_b$ as estimated R_a and R_b, and $l_i^{'}$ s is observer gain, respectively.

Remark 2: Note that adding $L_{ob}C\left(x-\hat{x}\right)$ to $A(\theta)\hat{x}$ results in making system matrix, $\tilde{A}(\theta) = A(\theta) - L_{ob}C$, become skew symmetric. Thus the nonlinear observer dynamics can become passive system with the observer gain, $l_\theta > 0$, $l_\omega = L/J$, $l_a > 0$, $l_b > 0$. ♦

L_{ob} should be designed so that $\tilde{A}(\theta)$ is Hurwitz. If $l_\theta > 0$, $l_\omega = L/J$, $l_a > 0$, $l_b > 0$, then $\tilde{A}(\theta)$ is Hurwitz, regardless of θ. The estimation states error, $\tilde{x} = x - \hat{x}$, and the estimation resistance errors, $\tilde{R}_a = R_a - \hat{R}_a$, $\tilde{R}_b = R_b - \hat{R}_b$, are defined. Theorem 3 shows that $\tilde{x}$, $\tilde{R}_a$, and $\tilde{R}_b$ converge to 0.

Theorem 3: Consider the error dynamics as

$$\dot{\tilde{x}} = \tilde{A}(\theta)\tilde{x} + \phi_a\left(i_a\right)\tilde{R}_a + \phi_b\left(i_b\right)\tilde{R}_b. \tag{15}$$

If the adaptive laws are designed as

$$\dot{\hat{R}}_a = -\frac{\gamma_a}{L}\tilde{i}_a i_a \tag{16}$$

$$\dot{\hat{R}}_b = -\frac{\gamma_b}{L}\tilde{i}_b i_b \tag{17}$$

and the persistently exciting conditions (PEs) as

$$\int_t^{t+T_a}\left(\tilde{i}_a(\tau)i_a(\tau)\right)^2 d\tau > 0 \tag{18}$$

$$\int_t^{t+T_b}\left(\tilde{i}_b(\tau)i_b(\tau)\right)^2 d\tau > 0 \tag{19}$$

for all $t \geq 0$, some finite Taand Tbare satisfied, then $\tilde{x} \rightarrow 0$, $\tilde{R}_a \rightarrow 0$, and $\tilde{R}_b \rightarrow 0$ as $t \rightarrow \infty$. ♦

Proof: The Lyapunov candidate function V_2 is defined as

$$V_2 = \frac{1}{2}\tilde{x}^T P_2 \tilde{x} + \frac{1}{2\gamma_a}\tilde{R}_a^2 + \frac{1}{2\gamma_b}\tilde{R}_b^2 \tag{20}$$

where

$$P_2 = \begin{bmatrix} 1 & 0 & 0 & 0 \\ 0 & \frac{J}{L} & 0 & 0 \\ 0 & 0 & 1 & 0 \\ 0 & 0 & 0 & 1 \end{bmatrix}.$$

The derivative of V_2 is given as

$$\begin{aligned} \dot{V}_2 = &-\frac{1}{2}\tilde{x}^T Q_2 \tilde{x} + \tilde{x}^T P_2 \phi_a(i_a)\tilde{R}_a + \tilde{x}^T P_2 \phi_b(i_b)\tilde{R}_b \\ &+ \frac{1}{\gamma_a}\dot{\tilde{R}}_a \tilde{R}_a + \frac{1}{\gamma_b}\dot{\tilde{R}}_b \tilde{R}_b \end{aligned} \tag{21}$$

where

$$\begin{aligned} Q_2 &= -\frac{1}{2}\left(P_2 \tilde{A}(\theta) + \tilde{A}^T(\theta) P_2\right) \\ &= \begin{bmatrix} l_\theta & 0 & 0 & 0 \\ 0 & \frac{B}{L} & 0 & 0 \\ 0 & 0 & l_a & 0 \\ 0 & 0 & 0 & l_b \end{bmatrix} \end{aligned}$$

$\dot{\tilde{R}}_a = -\dot{\hat{R}}_a$, and $\dot{\tilde{R}}_b = -\dot{\hat{R}}_b$. Taking $\dot{\tilde{R}}_a = -\gamma_a \tilde{x}^T P_2 \phi_a(i_a)$ and $\dot{\tilde{R}}_b = -\gamma_b \tilde{x}^T P_2 \phi_b(i_b)$ gives us $\dot{V}_2$ as follows

$$\dot{V}_2 = -\tilde{x}^T Q_2 \tilde{x}. \tag{22}$$

Therefore, $V_2(t) \in L_\infty$. Thus $\tilde{x} \in L_\infty$, $\tilde{R}_a \in L_\infty$ and $\tilde{R}_b \in L_\infty$. Integrating (22) gives

$$V_2(t) - V_2(0) = -\int_0^t \tilde{x}^T(\tau) Q_2 \tilde{x}(\tau) d\tau. \tag{23}$$

Since $V_2(t) \in L_2$ and $V_2(0)$ are finite, $\tilde{x} \in L_2$. From (15), $\dot{\tilde{x}} \in L_\infty$. Therefore, $\tilde{x} \to 0$ based on Barbalat's lemma [27]. Also from (15), $\dot{\tilde{x}}$ is uniformly continuous. By Barbalat's lemma [27], we also conclude that $\dot{\tilde{x}} \to 0$. Thus, if the PEs (18),(19) are satisfied, then $\tilde{R}_a \to 0$ and $\tilde{R}_b \to 0$. ■

As long as PM stepper motor keeps rotating, the PEs (18), (19) are always satisfied. Then, the zero equilibrium point of the error dynamics (15) are uniformly asymptotically stable.

4. Closed-loop System Stability Analysis

Since ω, R_a, and R_b are unknown, the desired phase currents (7) and the desired current errors (8) should be modified respectively such as

$$\hat{i}_a^d = \frac{2V_{\max}}{\hat{R}_a + \hat{R}_b}\cos(N_r\theta^d), \hat{i}_b^d = \frac{2V_{\max}}{\hat{R}_a + \hat{R}_b}\sin(N_r\theta^d) \tag{24}$$

and

$$\begin{aligned} \hat{e}_{a_I}(t) &= \int_0^t \hat{e}_a(\tau)d\tau,\ \hat{e}_a(t) = \hat{i}_a^d(t) - i_a \\ \hat{e}_{b_I}(t) &= \int_0^t \hat{e}_b(\tau)d\tau,\ \hat{e}_b(t) = \hat{i}_b^d(t) - i_b. \end{aligned} \tag{25}$$

Therefore, the control law (9) needs to be modified to cancel the additional terms, $\dot{\hat{R}}_a i_a$ and $\dot{\hat{R}}_b i_b$ as

$$\begin{aligned} v_a &= \left(\hat{R}_a i_a - K_m \hat{\omega}\sin(N_r\theta)\right) + L\left(\dot{\hat{i}}_a^d + \rho_{a_I}\hat{e}_{a_I} + \rho_a \hat{e}_a\right) \\ v_b &= \left(\hat{R}_b i_b + K_m \hat{\omega}\cos(N_r\theta)\right) + L\left(\dot{\hat{i}}_b^d + \rho_{b_I}\hat{e}_{b_I} + \rho_b \hat{e}_b\right). \end{aligned} \tag{26}$$

Due to the estimated errors (25) and the modified control law (26), the estimated error dynamics are given by

$$\begin{aligned} \dot{\hat{e}}_a &= -\rho_a \hat{e}_a + \frac{1}{L}\left(\tilde{R}_a i_a + K_m \tilde{\omega}\sin(N_r\theta)\right) \\ \dot{\hat{e}}_b &= -\rho_b \hat{e}_b + \frac{1}{L}\left(\tilde{R}_b i_b - K_m \tilde{\omega}\cos(N_r\theta)\right). \end{aligned} \tag{27}$$

From (15), (16), (17), and (27), we obtain the closed-loop system as

$$\begin{aligned} \dot{\hat{e}}_{a_I} &= \hat{e}_a \\ \dot{\hat{e}}_a &= -\rho_{a_I}\hat{e}_{a_I} - \rho_a \hat{e}_a + \frac{K_m \sin(N_r\theta)}{L}\tilde{\omega} + \frac{i_a}{L}\tilde{R}_a \\ \dot{\hat{e}}_{b_I} &= \hat{e}_b \\ \dot{\hat{e}}_b &= -\rho_{b_I}\hat{e}_{b_I} - \rho_b \hat{e}_b - \frac{K_m \cos(N_r\theta)}{L}\tilde{\omega} + \frac{i_b}{L}\tilde{R}_b \\ \dot{\tilde{\theta}} &= -l_\theta \tilde{\theta} + \tilde{\omega} \\ \dot{\tilde{\omega}} &= -\frac{L}{J}\tilde{\theta} - \frac{B}{J}\tilde{\omega} - \frac{K_m}{J}\sin(N_r\theta)\tilde{i}_a + \frac{K_m}{J}\cos(N_r\theta)\tilde{i}_b \\ \dot{\tilde{i}}_a &= \frac{K_m}{L}\sin(N_r\theta)\tilde{\omega} - l_a \tilde{i}_a - \frac{i_a}{L}\tilde{R}_a \\ \dot{\tilde{i}}_b &= -\frac{K_m}{L}\cos(N_r\theta)\tilde{\omega} - l_b \tilde{i}_b - \frac{i_b}{L}\tilde{R}_b \\ \dot{\hat{R}}_a &= \frac{\gamma_a}{L} i_a \tilde{i}_a \\ \dot{\hat{R}}_b &= \frac{\gamma_b}{L} i_b \tilde{i}_b. \end{aligned} \tag{28}$$

Theorem 4: Consider the closed-loop system (28). If PEs (18), (19) are satisfied, then $\hat{e}_a$, $\hat{e}_b$, $\tilde{x}$, $\tilde{R}_a$ and $\tilde{R}_b$ approach zero as $t \to \infty$. Thus, e_{a_1}, e_a, e_{b_1}, and e_b go to zero as $t \to \infty$. ♦

Proof: The closed-loop system (28) can be rewritten as

$$\begin{aligned} \dot{\psi}_1 &= A_{\psi_1}\psi_1 + B_{\psi_1}(x)\psi_2 \\ \dot{\psi}_2 &= A_{\psi_2}(x)\psi_2 \end{aligned} \tag{29}$$

where $\psi_1 = \left[\hat{e}_{a_1}, \hat{e}_a, \hat{e}_{b_1}, \hat{e}_b\right]^T$, $\psi_2 = \left[\tilde{x}^T, \tilde{R}_a, \tilde{R}_b\right]^T$

$$A_{\psi_1} = \begin{bmatrix} 0 & 1 & 0 & 0 \\ -\rho_{a_1} & -\rho_a & 0 & 0 \\ 0 & 0 & 0 & 1 \\ 0 & 0 & -\rho_{b_1} & -\rho_b \end{bmatrix}$$

$$B_{\psi_1}(x) = \begin{bmatrix} 0 & 0 & 0 & 0 & 0 & 0 \\ 0 & \frac{K_m S}{L} & 0 & 0 & \frac{\hat{R}_a i_a}{L} & 0 \\ 0 & 0 & 0 & 0 & 0 & 0 \\ 0 & -\frac{K_m C}{L} & 0 & 0 & 0 & \frac{\hat{R}_b i_b}{L} \end{bmatrix}$$

$$A_{\psi_2}(x) = \begin{bmatrix} -l_\theta & 1 & 0 & 0 & 0 & 0 \\ -\frac{L}{J} & -\frac{B}{J} & -\frac{K_m}{J}S & \frac{K_m}{J}C & 0 & 0 \\ 0 & \frac{K_m}{L}S & -l_a & 0 & -\frac{i_a}{L} & 0 \\ 0 & -\frac{K_m}{L}C & 0 & -l_b & 0 & -\frac{i_b}{L} \\ 0 & 0 & \frac{\gamma_a}{L}i_a & 0 & 0 & 0 \\ 0 & 0 & 0 & \frac{\gamma_b}{L}i_b & 0 & 0 \end{bmatrix}$$

$S = \sin(N_r\theta)$ and $C = \cos(N_r\theta)$, respectively. Note that A_{ψ_1} is Hurwitz and $B_{\psi_1}(x)$ is uniformly bounded. Therefore, the dynamics of ψ_1 is input to state stable [25]. In Section 3, it was shown that ψ_2 goes to zero as $t \to \infty$ if PEs (18), (19) are satisfied. Therefore ψ_1 goes to zero as $t \to \infty$. e_a and e_b are

$$\begin{aligned} e_a &= i_a^d - i_a \\ &= \hat{e}_a + \tilde{i}_a^d \\ e_b &= i_b^d - i_b \\ &= \hat{e}_b + \tilde{i}_b^d \end{aligned} \tag{30}$$

where $\tilde{i}_a^d = -\frac{2V_{\max}\left(\tilde{R}_a + \tilde{R}_b\right)}{\left(R_a + R_b\right)\left(\hat{R}_a + \hat{R}_b\right)}\cos\left(N_r\theta^d\right)$ and

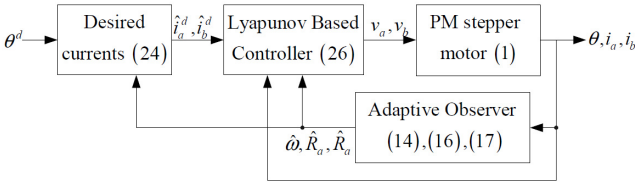

Fig. 4. Block diagram of the controller structure

$\tilde{i}_b^d = -\frac{2V_{\max}\left(\tilde{R}_a + \tilde{R}_b\right)}{\left(R_a + R_b\right)\left(\hat{R}_a + \hat{R}_b\right)}\sin\left(N_r\theta^d\right)$. Since $\hat{e}_a$, $\hat{e}_b$, $\tilde{x}$, $\tilde{R}_a$, and $\tilde{R}_b$ approach zero as $t \to \infty$, e_{a_1}, e_a, e_{b_1}, and e_b go to zero.

Fig. 4 shows the block diagram of the controller structure. The adaptive observer estimates the velocity and the phase resistances. Then, the compensative microstepping generates the desired currents using the estimated resistances. Finally, the Lyapunov based controller makes the actual control inputs.

5. Simulation Results

Simulations were performed to evaluate the performance of the proposed controller. The PM stepper motor model consisting of SimScape models was used. For the implementation of the proposed method, the S-function coded in C language was used. The measurement noises in the current sensor had 0.05 A of the maximum ranges. The dc offset in the current sensor was 0.01 A. The parameters in Table I and the reference position shown in Fig. 2 were used. The control parameters are listed in Table II. For the validation of the proposed method, simulations for two cases were used:

[Case 1] the microstepping based nonlinear control [12]

$$\begin{aligned} i_a^d &= \frac{V_{\max}}{R}\cos\left(N_r\theta^d\right) \\ i_b^d &= \frac{V_{\max}}{R}\sin\left(N_r\theta^d\right) \\ v_a &= \left(R_a i_a - K_m\omega\sin\left(N_r\theta\right)\right) + L\left(\dot{i}_a^d + \rho_{a_1}e_{a_1} + \rho_a e_a\right) \\ v_b &= \left(R_b i_b + K_m\omega\cos\left(N_r\theta\right)\right) + L\left(\dot{i}_b^d + \rho_{b_1}e_{b_1} + \rho_b e_b\right) \end{aligned} \tag{31}$$

and [Case 2] the compensative microstepping based control with the passive nonlinear adaptive observer

$$\begin{aligned} \hat{i}_a^d &= \frac{2V_{\max}}{\hat{R}_a + \hat{R}_b}\cos\left(N_r\theta^d\right) \\ \hat{i}_b^d &= \frac{2V_{\max}}{\hat{R}_a + \hat{R}_b}\sin\left(N_r\theta^d\right) \\ v_a &= \left(\hat{R}_a i_a - K_m\hat{\omega}\sin\left(N_r\theta\right)\right) + L\left(\dot{\hat{i}}_a^d + \rho_{a_1}\hat{e}_{a_1} + \rho_a\hat{e}_a\right) \end{aligned}$$

$$
\begin{aligned}
v_b &= \left(\hat{R}_b i_b + K_m \hat{\omega}\cos\left(N_r\theta\right)\right) + L\left(\dot{\hat{i}}_b^d + \rho_{b_i}\hat{e}_{b_i} + \rho_b \hat{e}_b\right) \\
\dot{\hat{x}} &= A(\theta)\hat{x} + \phi_a\left(i_a\right)\hat{R}_a + \phi_b\left(i_b\right)\hat{R}_b + Bu + L_{ob}C\left(x-\hat{x}\right) \\
\dot{\hat{R}}_a &= -\frac{\gamma_a}{L}\tilde{i}_a i_a \\
\dot{\hat{R}}_b &= -\frac{\gamma_b}{L}\tilde{i}_b i_b
\end{aligned} \tag{32}
$$

In case 1, the controller based on previous microstepping [12] is used. The nominal resistance R was used to make the Lissajou curve of the desired current become circle instead of the actual phase resistance, R_a and R_b. In case 2, the proposed controller based on compensative microstepping with passive nonlinear adaptive observer is used.

5.1. Comparison of the microstepping and the compensative microstepping

Fig. 5 shows the position tracking errors of both cases. The high frequency components of the position ripples were unavoidable due to the PWM drivers and the current measurement noise. As the simulation results shown in Fig. 3(a), the proposed method using the compensative microstepping can reduce the position ripple. The steady-state position error was unobservable due to the position ripple increased due to PWM drivers and the current measurement noise. The Lissajou curves of the phase currents of both methods are shown in Fig. 6. The Lissajou curves of the phase currents for both cases and the desired currents are shown in Fig. 6. The Lissajou curve of the phase of case 1 seems to be nearly circles as shown in Fig. 6. Note that the Lissajou curve of the phase currents of the case 1 was slightly ellipse due to the asymmetric measurement noises in the phase A and B However, the Lissajou curve of the phase currents of the case 1 was ellipse as shown in Figs. 6. Thus the position error in the steady-state and the ripple were observed in the case 1. On the other hand, the Lissajou curve of the phase currents of the case 2 was nearly circle as shown in Fig. 6 so that the position ripple can be reduced.

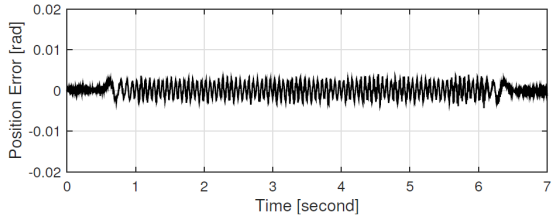

(a) Case 1

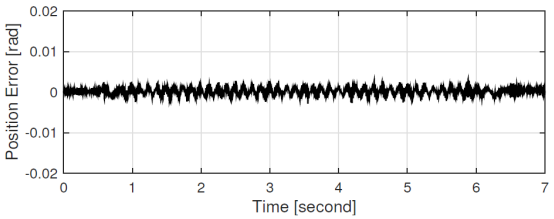

(b) Case 2

Fig. 5. Position tracking errors of cases 1 and 2

5.2. Evaluation of the proposed nonlinear adaptive observer and controller

Figs. 7 and 8 show the estimation results of the velocity and the phase resistances in case 2. $\hat{\omega}$, $\hat{R}_a$, and $\hat{R}_b$ tracked the real values ω, R_a, and R_b. However, since PE

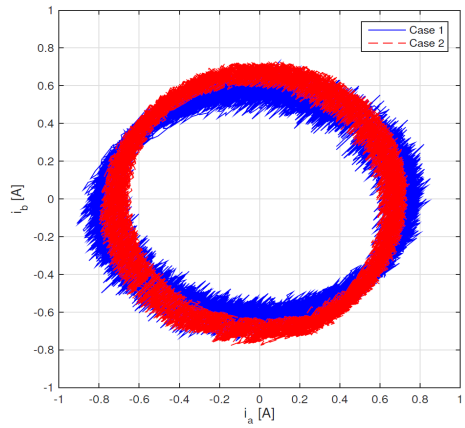

Fig. 6. Lissajou curve of the phase currents of the both methods

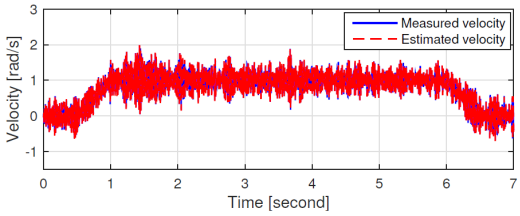

Fig. 7. Estimation of the velocity of case 2

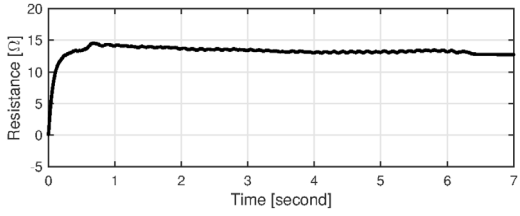

(a) $\hat{R}_a$ with $\hat{R}_a(0)=0$

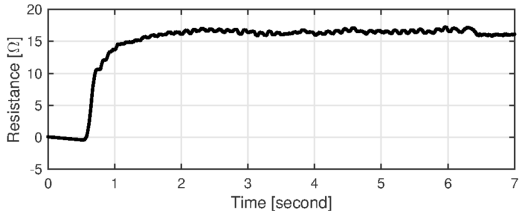

(b) $\hat{R}_b$ with $\hat{R}_b(0)=0$

Fig. 8. Estimations of the phase resistances of case 2

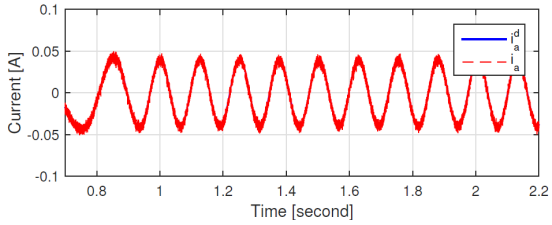

(a) Current tracking performance in phase A

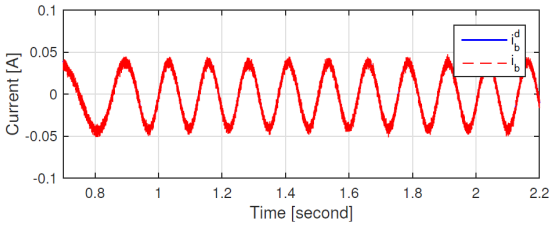

(b) Current tracking performance in phase B

Fig. 9. Current tracking performance of case 2

(19) was not satisfied at the outset ($0 \leq t < 0.2$s), i.e., before rotation of PM stepper motor, $\hat{R}_b$ does not converge to R_b. The current tracking performances are shown in Fig. 9. The amplitudes of the phase currents of the controller with the compensative microstepping were not decreased and did not have the phase lag by the proposed controller.

6. Conclusions

In this paper, nonlinear adaptive control with compensative microstepping was proposed. The desired voltage inputs of microstepping were modified to enforce the Lissajou of the desired phase currents to form a circle when the resistances in phases A and B were different. To allow the phase currents to follow the desired phase currents during operation, the Lyapunov-based controller was modified. An adaptive observer was designed to estimate the velocity and phase resistances. The stability of the closed-loop was proven using passivity. Simulation results showed that the steady-state position error disappeared when using the proposed method. The position ripple was also reduced during operation through the use of the proposed method. Furthermore, the resulting Lissajou curve of the phase currents was a circle.

Acknowledgements

This Research was supported by the Chung-Ang University Research Grants in 2016. This work was supported by the Industrial Source Technology Development Program (10044620, Automatic lane change system for novice drivers) funded by the Ministry of Trade, Industry and Energy (MOTIE, Korea).

References

[1] T. Kenjo, Stepping Motors and Their Microprocessor Control. New York:Clarendon, 1984.

[2] M. Bodson, J. S. Sato, and S. R. Silver, "Spontaneous Speed Reversals in Stepper Motors," *IEEE Trans. Control Syst. Technol.*, vol. 14, no. 2, pp. 369-273, Mar. 2006.

[3] D. W. Jones, "Control of stepping motors," Handbook of Small Electric Motors, W. H. Yeadon and A. W. Yeadon, Eds. McGraw-Hill, New York, 2001.

[4] Core techonologies. Motors and control systems for precise motion control. See also URL http://www.1-core.com/library/auto/motion-control/

[5] Manea, S., 2009. "Stepper motor control with dsPIC DSCs," Microchip Application Note, 1-26.

[6] A. Bellini, C. Concari, G. Franceschini, and A. Toscani, "Mixed-Mode PWM for High-Performance Stepping Motors," *IEEE Trans. Ind. Electron.*, vol. 54, no. 6, pp. 3167-3177, Dec. 2007.

[7] Orientalmotor Basics of motion control. See also URL http://www.orientalmotor.com/products/ac-dc-step-motors/alphastep-overview.html

[8] Sanyo-Denki, 2 Phase Stepping Systems. See also URL http://www.sanyo-denki.com/Data/Servo/catalogs/F2ver1.pdf

[9] A. S. Ghafari and A. Alasty, "Design and real-time experimental im-plementation of gain scheduling PID fuzzy controller for hybrid stepper motor in micro-step operation," *in Proc. IEEE Int. Conf. Mechatronics*, 2004, pp. 421-426.

[10] A. S. Ghafari and M. Behzad, "Investigation of the micro-step control positioning system performance affected by random input signals," *Mechatronics*, vol. 15, no. 10, pp. 1175-1189, 2005.

[11] W. Kim, I. Choi, K. Bae, and C. C. Chung, "A Lyapunov Method in Microstepping Control for Permanent Magnet Stepper Motors," *in Proc. IEEE Int. Conf. Mechatronics*, 2009, pp. 1-5.

[12] W. Kim, D. Shin, and C. C. Chung, "The Lyapunov-based controller with a passive nonlinear observer to improve position tracking performance of micro-stepping in permanent magnet stepper motors," *Automatica*, vol. 48, no. 12, pp. 3064-3074, 2012.

[13] W. Kim, D. Shin, and C. C. Chung, "Microstepping Using a Disturbance Observer and a Variable Structure Controller for Permanent Magnet Stepper Motors," *IEEE Trans. Ind. Electron.*, vol. 60, no. 7, pp. 2689-2699, 2013.

[14] W. Kim, D. Shin, Y. Lee, and C .C. Chung, "Micro-stepping with nonlinear torque modulation for permanent magnet stepper motors," *IEEE Trans. Control Syst. Technol.*, vol. 21, no. 5, pp. 1971-1979, 2013.

[15] D. Shin, W. Kim, Y. Lee, and C .C. Chung, "Phase compensation microstepping for permanent magnet

stepper motors," *IEEE Trans. Ind. Electron.*, vol. 60, no. 12, pp. 5773-5780, 2013.
[16] M. Bendjedia, Y. A. Amirat, B. Walther, and A. Berthon, "Position control of a sensorless stepper motor," *IEEE Trans. Power Electron*., vol. 27, no. 2, pp. 578-587, 2012.
[17] R. Delpoux and T. Floquet, "High-order sliding mode control for sensorless trajectory tracking of a PMSM," *Int. J. Control*, vol. 87, no. 10, pp. 2140-2155, 2014.
[18] Autonics, Stepper Motor Datasheet. See also URL http://www.autonics.com/upload/data/AK-2(KE-10-0020A).pdf
[19] R. Marino, S. Peresada, and P. Tomei, "Nonlinear Adaptive Control of Permanent Magnet Step Motors," Automatica, vol. 31, no. 11, pp. 1595-1604, 1995.
[20] Y. M. Cho and R. Rajamani "A systematic approach to adaptive observer synthesis for nonlinear systems." *IEEE Trans. Autom. Control*, vol. 42, no. 4, pp. 534-537, 1997.
[21] F. Khorrami, P. Krishnamurthy, P, and H. Melkote, H., Modeling and Adaptive Nonlinear Control of Electric Motors, Heidelberg: Springer Verlag, 2003.
[22] J. Chiasson, Modeling and High-Performance Control of Electric Machines, Hoboken, NJ: Wiley-Interscience, 2005.
[23] M. Bodson, J. Chiasson, R. Novotnak, and R. Ftekowski, "High-Performance Nonlinear Feedback Control of a Permanent Magnet Stepper Motor," *IEEE Trans. Control Syst. Technol*., vol. 1, no. 1, pp. 5-14, Mar. 1993.
[24] Orientalmotor, "PK Series Stepping Motors," Hampshire, U.K. [Online]. Available: http://www.orientalmotor.com/ products/pdfs/2012-2013/A/usa st 09 1.8 pk motor only.pdf
[25] H. Khalil, Nonlinear Systems, 3rd ed. Upper Saddle River, NJ: Prentice-Hall, 2002.
[26] R. Kosut, "Design of linear systems with saturating linear control and bounded states," *IEEE Trans. Automat. Control*, vol. 28, no. 1, pp. 121-124, 1983.
[27] P. A. Ioannou and J. Sun, Robust Adaptive Control, Englewood Cliffs, NJ: Prentice-Hall, 1996.

Wonhee Kim He received the B.S. and M.S. degrees in electrical computer engineering, and the Ph.D. degree in electrical engineering from Hanyang University, Seoul, South Korea, in 2003, 2005, and 2012, respectively. He is currently an Assistant Professor with the School of Energy Systems Engineering, Chung-Ang University, Seoul. From 2005 to 2007, he was at Samsung Electronics Company, Suwon, South Korea. In 2012, he was at the Power and Industrial Systems Research and Development Center, Hyosung Corporation, Seoul. In 2013, he was a Postdoctoral Researcher at the Institute of Nano Science and Technology, Hanyang University, and a Visiting Scholar in the Department of Mechanical Engineering, University of California, Berkeley, CA, USA. From 2014 to 2016, he was in the Department of Electrical Engineering, Dong-A University, Busan, South Korea. His current research interests include nonlinear control and nonlinear observers, as well as their industrial applications.

Youngwoo Lee He received the B.S. in electrical engineering from Chungbuk National University, Cheongju, South Korea, and the Ph.D. degree in electrical engineering from Hanyang University, Seoul, South Korea in 2010 and 2017. Currently, Dr. Lee is a Post-Doctoral Researcher with School of Electrical and Computer Engineering in Ulsan National Institute of Science and Technology, Ulsan, South Korea, and a Visiting Scholar with the Department of Mechanical Engineering, University of California, Berkeley, CA, USA. His current research interests include nonlinear and optimal controller design. Dr. Lee is a member of the Institute of Electrical and Electronics Engineers, the Institute of Control, Robotics and Systems, and the Korean Institute of Electrical Engineers.

Donghoon Shin He received the B.S. degree in electrical computer engineering and the Ph.D. degree in electrical engineering from Hanyang University, Seoul, South Korea, in 2009 and 2016, respectively. He is currently a Senior Research Engineer with the Global Research and Development Center, Mando Corporation, Seongnam, South Korea. His research interests include nonlinear control and observer, as well as their industrial applications. Dr. Shin is a member of the Institute of Control, Robotics, and Systems, and the Korean Institute of Electrical Engineers.

Chung Choo Chung He received the B.S. and M.S. degrees in electrical engineering from Seoul National University, Seoul, South Korea, and the Ph.D. degree in electrical and computer engineering from the University of Southern California, Los Angeles, CA, USA, in 1993. From 1994 to 1997, he was with the Samsung Advanced Institute of Technology, Korea. In 1997, he joined the Faculty of Hanyang University, Seoul, South Korea. He was an Associate

Editor of the Asian Journal of Control from 2000 to 2002 and an Editor of the International Journal of Control, Automation and Systems from 2003 to 2005. He served an Associate Editor for various international conferences, such as the IEEE Conference on Decision and Control (CDC), the American Control Conferences, the IEEE Intelligent Vehicles Symposium, the Intelligent Transportation Systems Conference. He was a Guest Editor of the special issue on advanced servo control for emerging data storage systems published by the IEEE Transactions on Control System Technologies (TCST). He is currently an Associate Editor of TCST, the IEEE Transactions on Intelligent Transportation Systems, and the IFAC Mechatronics, and a Guest Editor of the IEEE Intelligent Transportation Systems Magazine. Dr. Chung was an Organizing Chair of the International Conference on Control, Automation and Systems 2011 and a Program Co-Chair of the 2015 IEEE Intelligent Vehicles Symposium. He is currently a General Co-Chair of CDC 2020 to be held in Korea with Prof. Braatz of MIT.